CRITICAL REVIEW

Review on mid-spatial frequency error suppression in optical components manufacturing

Yonghong Deng[1,2,3] · Xi Hou[1] · Bincheng Li[2] · Jia Wang[1] · Yun Zhang[1]

Abstract

With the growing prosperity of optical systems, the demand for high-precision optical components is becoming increasingly urgent. The mid-spatial frequency error generated on the optical components surface during the manufacturing process has become a bottleneck that restricts the improvement of the manufacturing accuracy of optical components. In this review, the processing techniques and polishing principles for optical components manufacturing are first briefly described and the source of mid-spatial frequency error is analyzed in detail. Then, several widely adopted suppression techniques in optical components manufacturing for mid-spatial frequency error are introduced in detail, such as the optimization methods for polishing path and polishing tool structure, and ion beam layer removal method. Moreover, their basic concepts, polishing mechanisms, development history, and characteristics are presented. Finally, the development of suppression techniques of mid-spatial frequency error for optical polishing is summarized and prospected. This paper analyses the problems of mid-spatial frequency error in optical components manufacturing, which may be worth investigating in the future.

Keywords Optical polishing · Mid-spatial frequency error · Smoothing tool · Ultra-precision polishing

1 Introduction

Optical components are widely adopted in optical imaging, space observation, and other fields. With the rapid development of technology in these application fields, much higher performance of optical components is required. Thereby, the demand for ultra-precision surface manufacturing of optical components is becoming more urgent [1–3]. The current ultra-precision optical component processing chain is shown in Fig. 1. First, the surface of a component is processed to the closest spherical surface by computer numerical control machine tools (CNC) machines or robots, and the machining accuracy of the component surface is within several micrometers. Second, the closest spherical surface of the component is ground to an aspherical surface by ultra-precision CNC machines or robots, and the accuracy of the aspherical surface reaches around a few tenths of a micrometer. Third, the surface is polished by a small size grinding head or a bonnet tool, and the roughness of the component surface is reduced to tens of nanometers. Fourth, the surface is smoothed by a pitch tool, and its accuracy is further improved to within about ten nanometers. Finally, the surface is further figured by ion beam polishing; then, its accuracy is achieved to a few nanometers or even a few tenths of a nanometer [4, 5].

Currently, although the optical manufacturing technology has made progress and makes the manufacturing accuracy of optical component surface continue to improve, it is still a serious technical challenge to reduce the manufacturing error of optical components. Therefore, how to improve the manufacturing accuracy of optical component is a hot and difficult problem.

According to the international standards for the quality evaluation of optical components, wavefront root mean square (RMS), peak-to-valley (PV), Zernike polynomial, and PSD are currently used as evaluation metrics for optical components. James et al. [6] divided the surface shape error into three regimes based on the power spectral density (PSD) and spatial frequency, which are low spatial frequency

✉ Xi Hou
  houxi@ioe.ac.cn

1 Institute of Optics and Electronics, Chinese Academy of Sciences, Chengdu 610209, China

2 School of Optoelectronic Science and Engineering, University of Electronic Science and Technology of China, Chengdu 610054, China

3 University of Chinese Academy of Sciences, Beijing 100049, China

Fig. 1 The ultra-precision optical component processing chain

Main processing technology
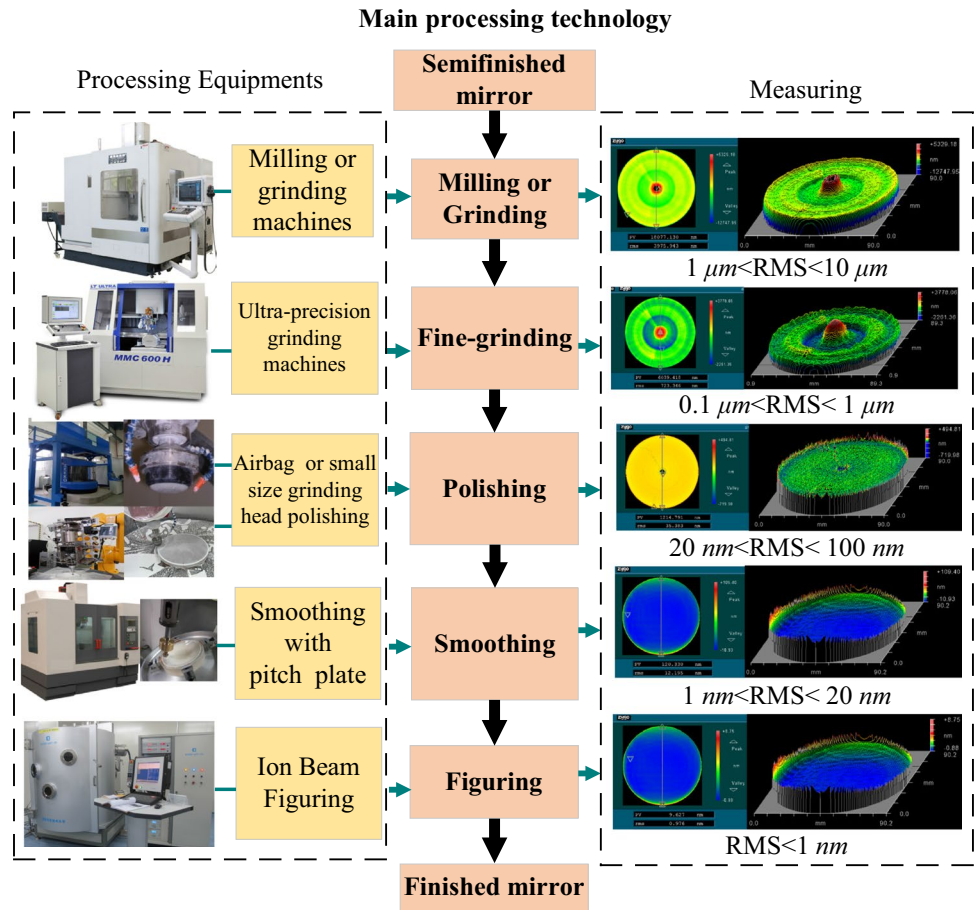
surface error (LSF), mid spatial frequency ripple (MSF), and high spatial frequency microroughness (HSF), respectively. The scattering effects from each spatial frequency regime are as shown in Fig. 2. The Lawrence Livermore National Laboratory in the USA adopted PSD to characterize the MSF and HSF errors of bright parts in the National Ignition Facility (NIF) and constructed a standard line for the surface error in the 0.03 to 8.33 mm^{-1} frequency band. Therefore,

the PSD term is applied to define the indicator of waviness and smoothness for the evaluation of the wavefront error of NIF optics.

In addition, the periodic spatial frequency characterizes the irregularity of the optical surface. The spatial frequency is divided into different frequency domains: it will be considered as the optical system's loss if the spatial frequency is high which is similar to the surface roughness. If the

Fig. 2 The error distribution regimes of optical components surface [6]
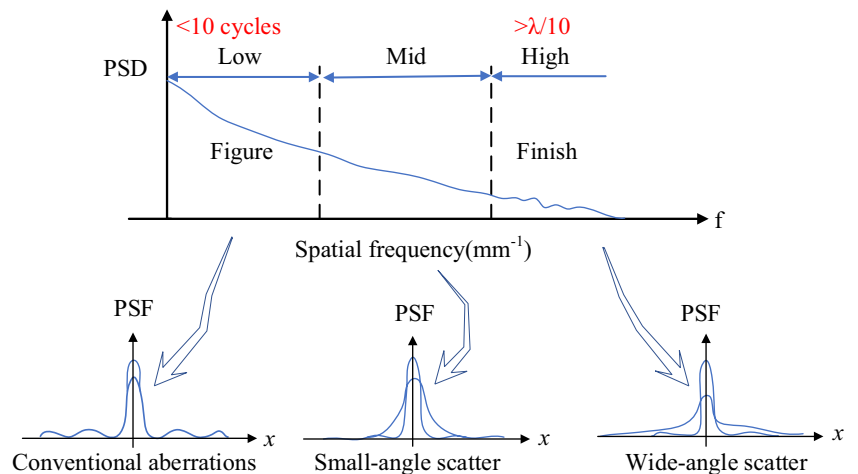
spatial frequency is low, the shape change can be expressed by methods such as Zernike polynomials for the low-frequency portion. When the spatial frequency is too high to be easily defined using polynomials (more than 10 periods are included in the aperture) or when the spatial frequency is too low to ignore its effects (The ripple period relative to the wavelength is greater than one-tenth of the optical path from the given surface to the image surface), it is collectively referred to as the mid-frequency portion.

Computer-controlled optical surface (CCOS) technique, bonnet polishing, magnetorheological finishing, etc., are frequently applied optical manufacturing techniques. They will inevitably generate MSF and HSF errors in the polishing process stage [7]. Although the LSF error can be easily eliminated nowadays, MSF and HSF errors are still difficult to be restrained. The existing MSF and HSF errors will seriously affect the image quality of optical imaging systems and the energy focusing of optical systems. Therefore, how to reduce the MSF error of optical components is a difficult problem to improve the performance of optical systems.

A detailed overview of the techniques and progress for restraining the MSF in optical components manufacturing is presented in this paper. The research contributions of this work contain:

(a) some basic concepts of optical components polishing are introduced, and the source of mid and high spatial frequency errors is presented.
(b) The methods for reducing MSF error are explained, which are polishing path optimization, structural optimization of polishing tools, ion beam layer removal, etc.; the current related research work is reviewed.
(c) Various problems of MSF error suppression in optical components manufacturing are discussed and new ideas for future research are provided.

The structure of this paper is as follows. Section 2 states some basic principles of polishing processing and the source of mid-spatial frequency error. Section 3 gives some classical suppression methods and their applications. Section 4 presents the discussions of suppression methods. Summarizes and prospect are drawn in Sect. 5.

2 The source of mid-spatial frequency errors

2.1 The basic principles of polishing processing

It is widely acknowledged that the Preston equation effectively describes the removal characteristics of material on workpiece surface [8]. Small-tool polishing [9–14], magnetorheological finishing [15–19], and ion-beam figuring [20–24] are all based on the sub-aperture polishing method, so they have the same or similar fundamental theories.

$$dz(x, y) = k \cdot v(x, y) \cdot p(x, y) \cdot dt \tag{1}$$

where $dz(x,y)$ is the depth of material removal at a certain point on component surface. k is a proportional constant, which is determined by all factors except speed and pressure. $v(x,y)$ is the instantaneous relative velocity between the polishing tool and the component at a certain point on component surface. $p(x,y)$ is the instantaneous pressure between the polishing tool and the component at a certain point on component surface.

2.2 The source analysis of mid-spatial frequency error

Generally, it is easy to obtain very high precision flat optical components. The processing of spherical components can be realized by rotating the polishing tool or workpiece around a certain axis; thus, high precision spherical components can also be easily gained. The processing method of the plat or spherical surface workpieces can be processed by the full-aperture processing method, and the processing process will not generate a large number of MSF error. In the precision improvement stage, the workpiece only needs to refine the low-frequency surface shape error by the ion beam polishing processing, and it is possible to obtain components with qualified full-band error surface. For aspheric components without rotary axis or freeform surface components, the relative motion between the polishing tool and the workpiece is driven by the numerical control machine tools or robot, which is an interpolated motion. The interpolation motion makes the actual polishing path deviate from the theoretical path, which will lead to uneven material removal, and eventually generate MSF error, as is shown in Fig. 3.

The optical processing system is a sophisticated system; the source of MSF error is not only the interpolation motion but also polishing speed, stability, and correction of removal function, polishing spot, positioning accuracy, etc., as shown in Fig. 4. The impact of its polishing process system on MSF error is shown in Table 1.

It can be seen from Fig. 4 and Table 1 that there are many sources of MSF error generated by the processing system when polishing aspheric or freeform surface components. So, it is difficult to obtain high precision of aspheric components or freeform surface components. Therefore, the aspheric or freeform surface components can only be processed by the sub-aperture processing method. The new MSF error will be introduced by the instability of the removal function and the superposition of the processing trajectory, which cannot be refined by the ion beam processing. Thereby, it is more difficult to obtain aspheric or

Fig. 3 The MSF error on optical surface is generated by processing equipment

Machine tool

Optical surface machining

Polishing robot

Ringed MSF error
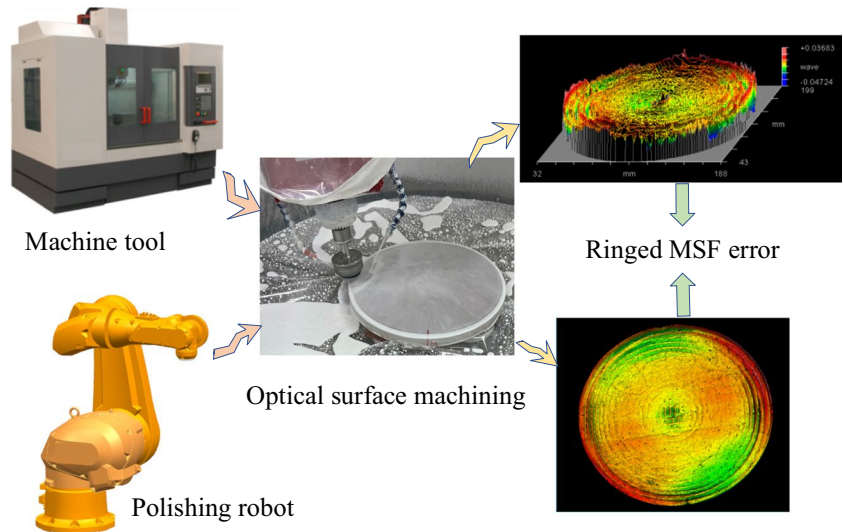
freeform surface components with higher surface accuracy than flat or spherical surface components with higher surface accuracy. Some factors in the polishing system are difficult to control, so we can only find effective ways to eliminate MSF error once they have been generated.

3 Methods for reducing the mid-spatial frequency ripple of component surface

3.1 Polishing path optimization methods for suppressing MSF error

It is widely believed that a reasonable polishing path can effectively improve the polishing quality of component surface. The optimal selection of the polishing path can decrease the movement stroke of polishing tool, slow down the movement speed and acceleration, cut down the equipment cost and processing cost, shorten the processing time, and improve the processing accuracy. A large number of literatures have shown that the polishing path can significantly reduce the ripple error of component surface, and the polishing path multi-directionality and direction randomness effectively suppress the MSF error caused by polishing. Single path and synthetic path are widely adopted polishing paths. Single paths include scan paths, spiral paths, concentric circle paths, and pseudo-random paths. A synthetic polishing path is typically a multidirectional composite polishing path, which mimics the manual polishing process by combining a single path with a sub-cycloid pattern. Especially, the application of different polishing paths is likely to result in differences in surface quality, fluctuations in machining efficiency, and changes in manufacturing costs. Researchers often optimize the polishing path to improve surface accuracy, which includes selecting the appropriate path type, calculating the path distribution, and setting the proper path spacing.

3.1.1 Simple polishing path

The simple polishing path is routinely adopted to polish some flat mirrors due to its simple generation algorithm and high polishing efficiency. Tam et al. [25] experimented with four tool paths, as shown in Fig. 5; then, they analyzed the characteristics
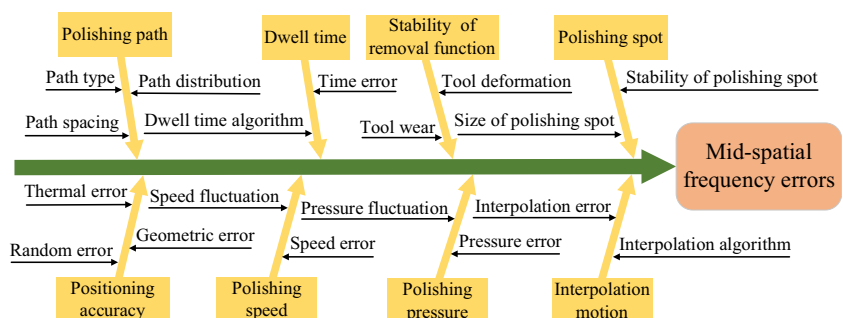
Fig. 4 The source of MSF error

Table 1 The impact of its polishing process system on MSF error

Error source	Impact
Interpolation motion	I. Interpolation algorithm: different interpolation algorithms can lead to different deviations between the real path and the theoretical path, which bring different MSF error
	II. Interpolation error: interpolation error is inevitable in the process of interpolation calculation. The larger the error of it, the larger the MSF error
Removal function	I. Tool wear: the contour of the removal function is changed due to abrasion of the polishing tool. The MSF error will be generated
	II. Tool deformation: the contour of the removal function is unstable due to the deformation of tool, the MSF error will be generated
Polishing spot	I. Size of polishing spot: the smaller the polishing spot, the stronger the shaping ability, but the MSF error will increase
	II. Stability of polishing spot: the greater the change of the size of the polishing point, the greater the MSF error
Polishing path	I. Path type: different path types such as linear and spiral paths, which have different directions of material removal, resulting in different size and distribution of the MSF error
	II. Path spacing: different sizes of path spacing generate different sizes of ripple residual errors
	III. Path distribution: the uniformity of the path distribution determines the size of the generated MSF error
Dwell time	I. Dwell time algorithm: the convergence accuracy obtained by different algorithms is different, resulting in different residual errors
	II. Time error: The lag or overrun of dwell time affects the amount of material removal
Polishing pressure	I. Pressure fluctuation: the pressure fluctuation causes uneven material removal, resulting in the MSF error
	II. Pressure error: The deviation of pressure causes uneven material removal, resulting in the MSF error
Polishing speed	I. Speed fluctuation: fluctuations in polishing speed cause uneven material removal, which generates the MSF error
	II. Speed error: Deviations in speed control or detection cause uneven material removal, resulting in MSF error
Positioning accuracy	I. Geometric error: geometric error causes deviation of polishing path, which will be the generation of the MSF error
	II. Thermal error: thermal drift causes the path of polishing head to shift, which will generate the MSF error
	III. Random error: random error causes the polishing path to fluctuate, which will generate the MSF error

of four tool paths for material removal. They obtained means to reduce roughness in polishing, which should make the direction change of tool path smooth and make the distribution of the tool path spacing uniform throughout the component surface. Subsequently, Tam et al. [26] proposed peano-like path, which was used for uniform removal material of aspherical component surface in polishing. They used the path to conduct

magnetorheological polishing experiments, and the surface roughness was significantly reduced to 0.91 nm.

3.1.2 Spiral polishing path

The spiral polishing path is also conventional applied in polishing, which is mainly used for polishing aspherical
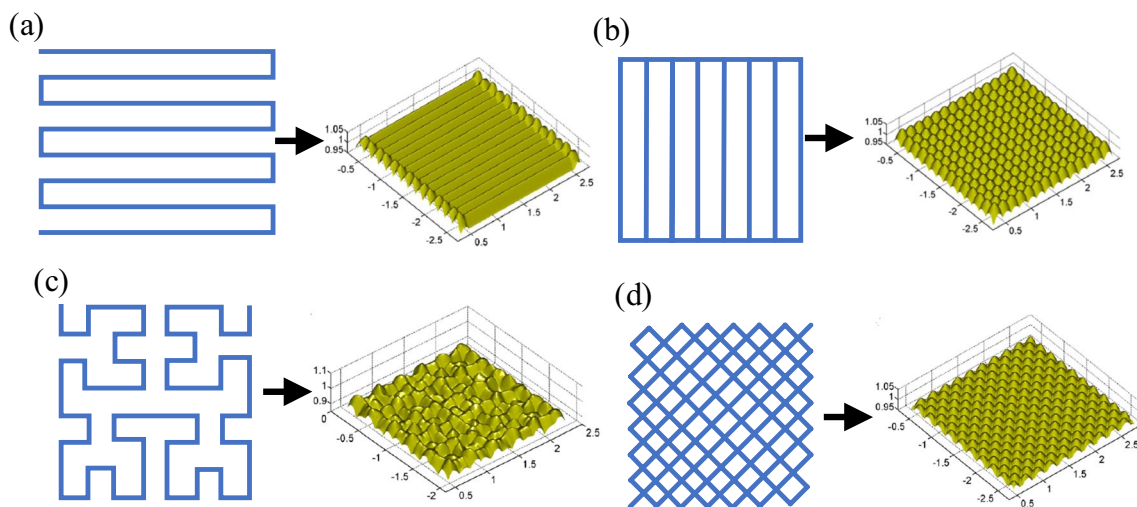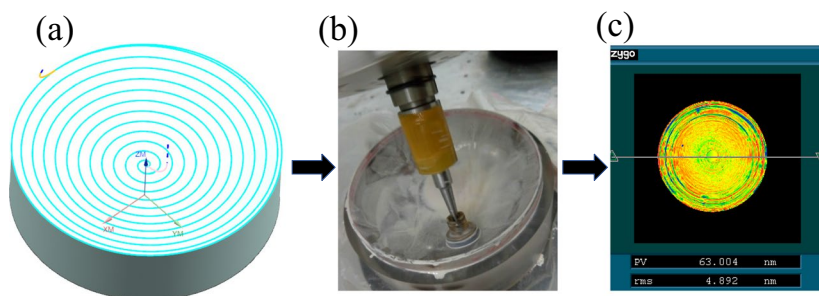

Fig. 5 Polishing paths for various styles [25]. **a** Scanning path, **b** bi-directional scanning path, **c** Hilbert path, and **d** Peano path. Copyright (2023) with permission from Elsevier

Fig. 6 3-D spiral path for the aspheric surface. **a** Diagram of spiral path generation, **b** spiral path polishing, and **c** spiral path polishing result

surfaces, as shown in Fig. 6. Many researchers have successfully used spiral paths to polish aspherical surfaces. Hauth et al. [27, 28] presented double-spiral polishing paths for polishing free-form surfaces, which can cover the whole surface. Then, they obtained high-precision surfaces through experiments. Feng et al. [29] designed a three-dimensional spiral path for reducing the ripple error of aspheric surfaces; its spacing is not affected by the curvature of the surface. The path can be uniformly distributed on aspheric surfaces. A variable pitch spiral path was proposed to reduce the figure error and MSF by Liu et al. [30] based on the characteristics of active feed polishing. The uniform removal of surface material had been achieved, and a high-precision surface had been obtained by using the path in the experiment. Hu et al. [31] used the random pitch spiral polishing path to restrict the residual error according to the distribution of error on the surface, and the surface accuracy of 0.059λ (RMS) was achieved through experiments. However, their choice of path spacing is based on empirical formulas, and the intrinsic relationship between shape error and path spacing has not been thoroughly investigated. Further, the spiral polishing path was generated through an iterative approximation algorithm by Han et al. [32, 33], which can achieve physical uniform coverage of the component surface, and reduce component surface roughness and profile errors. It can effectively avoid over-polishing and under-polishing, and obtain consistent surface quality. Zhao al. [34] used Archimedes spiral polishing path to achieve physical uniform coverage of aspheric surface. Qu et al. [35] proposed an optimized Archimedes spiral path, which can allow the material removal depth to remain consistent during the polishing process. Its effectiveness was proved, and a high-precision polished surface was obtained in experiments.

3.1.3 Pseudo-random polishing path

The pseudo-random path is proposed by Dunn et al. [36], which is utilized to restrict the MSF of aspheric surface in polishing, as shown in Fig. 7; they made a regular polishing path into an irregular polishing path. Pseudo-random processing path has the following typical characteristics. First, the polishing path is pre-defined by all discrete dwell points. Second, the polishing path passes through all discrete dwell points, but each point is passed only once. Third, the polishing path is non-self-intersecting. Fourth, the polishing path is a coherent route with spatial continuity, and it is an uninterrupted path. The spiral or regular raster scan path will create the regular CCOS convolutional residual errors. The pseudo-random polishing path can effectively reduce the CCOS convolutional residual error by changing the regularity and rhythmicity of the polishing path. Thereby, the MSF can be suppressed. The regular or periodic MSF error is randomly averaged by transforming the periodic polishing trajectory of the removal function into a chaotic scrambling line in processing.

The maximum entropy method based on the partial pseudo-random path was proposed by Dai et al. [37] in 2009, as shown in Fig. 8. They transformed the component surface into a series of discrete points in the MRF processing, as shown in Fig. 8a. a_i is a control area for polishing point action. c_i is a control point that drives the movement of the polishing spot, and l_k is a dwell points vector. Through research and analysis, they concluded that the MSF and HSF were strongly influenced by optical processing factors, which included initial surface
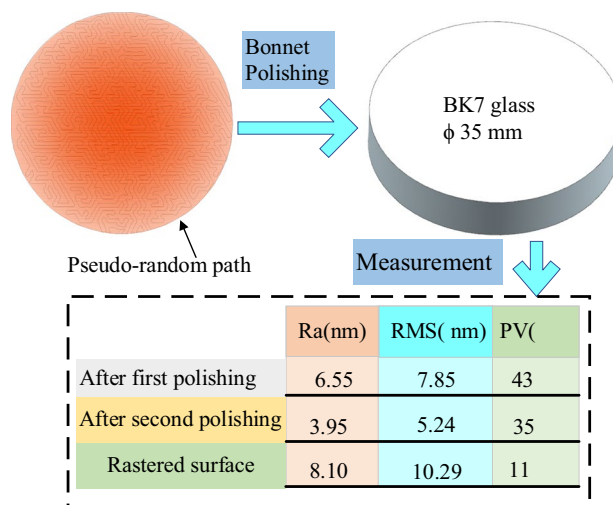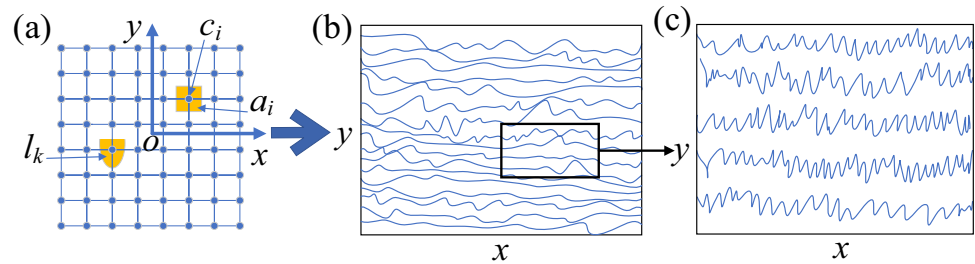

Fig. 7 Random polishing path for polishing [36]

	Ra(nm)	RMS(nm)	PV(
After first polishing	6.55	7.85	43
After second polishing	3.95	5.24	35
Rastered surface	8.10	10.29	11

Fig. 8 Part-random path generation [37]. **a** Discrete points of the component surface, **b** part-random path full figure, and **c** partially enlarged detail

shape, removal function, and polishing path planning. The initial surface shape of optical components mainly refers to the proportion of the initial surface shape error between the frequency domain and the spatial domain. The removal function primarily refers to the removal rate, cross-sectional profile, and stability of the removal function. The processing path planning is primarily to optimize the CCOS convolution residuals generated by the processing path. The information entropy theory was used to optical processing by them; the information entropy was used as a measure of random distribution of the resident points of removal function. A local random processing path is designed, and an experimental study is conducted to restrain the MSF and HSF errors. Its effectiveness was demonstrated. Wang et al. [38] presented a novel unicursal random maze polishing path with uniform coverage, which is random and multi-directional. They compared this path with the maze path, raster path, and Hilbert path in optical surface processing, and the results validate that this path can more effectively restrain the MSF error than other paths.

Subsequently, several researchers further investigated the pseudo-random path for polishing. Takizawa et al. [39] proposed a circular pseudorandom path to restrain the ripple error on polished surface, they compared this path with the raster path, the 4-direction path, and the 6-direction path through polishing experiments, and then studied the effect of various polishing tool feeds on surface accuracy. Their experimental results show that the circular pseudo-random path was obviously superior to other paths in polishing circular components. The random variation in the direction of the path and the change in polishing speed can strongly restrict the MSF error. Zhao et al. [40] proposed a B-splines pseudo-random polishing path based on the improved six-directional pseudorandom path, which can significantly improve the smoothness of the polishing path, and reduce the MSF error. Zha et al. [41] presented a polishing compensation method for polishing aspherical components based on the pseudo-random path, which can reduce the surface roughness and surface waviness, suppress the MSF error, and improve the surface quality of optical components in polishing experiments. There is a novel pseudo-random path generation method based on reconstructive points proposed

by Li et al. [42], which can entirely cover the components and can be efficiently generated with a large number of path points. The precision of the surface is 0.115λ (PV), and the MSF error can be significantly suppressed, as shown by experimental results. Beaucamp et al. [43] presented a circular-random path polishing for polishing aspheric and freeform optical components, which can entirely cover and uniformly distribute on the entire surface. The suppression of MSF error has a significant effective is shown in the polishing experiment.

3.1.4 Combine polishing paths and various optimizations based on paths

The application range of a single polishing path is limited, and it is difficult to meet the processing requirements of various components and the processing characteristics of diverse equipment. Therefore, a large number of researchers and engineers have optimized various aspects of the polishing path, synthesized multiple polishing paths, and combined them with other machining factors according to the processing characteristics of various equipment, the variability of the different process, and the shape of different components.

There is a piecewise-path convolution method based on the characteristic and the mechanism of the MSF error to predict the MSF error in polishing processing, which was presented by Wan et al. [44]. They have demonstrated the effectiveness of this method by applying it to zigzag paths, Archimedes spiral paths, and pseudo-random paths in numerical simulations and practical experiments to reduce MSF errors on the surface of optical elements, respectively. Han et al. [45] proposed a path optimization method based on surface shape error distribution; they constructed the corresponding relationship between residual error of the optical surface and polishing process parameters (such as material removal depth and path spacing). They achieved variable pitch polishing path by using this method based on the residual error distribution; it is better to maintain the polishing speed during the polishing process and provide the basis for dynamic control of the polishing process. Khakpour et al. [46] designed a uniform scanning path based on triangulated meshes of surfaces to polish free-form surfaces, and they analyzed the characteristics of freeform surfaces, such

as holes and complex boundaries. A constant offset distance can be obtained at anywhere on surfaces depending on the reference curve and specific directions, and the main path can also be discretized into sub-paths in abrasive waterjet polishing.

Simple path planning does not guarantee uniform removal of material, and it is limited to improve the surface accuracy. Rososhansky et al. [47] proposed a polishing path based on the contact status between the polishing tool and the workpiece to improve the surface quality. They built the contact area map using some discrete points on the polishing path, which can display the contact surface between the polishing tool and the workpiece during polishing, and identify under-polishing and over-polishing on the workpiece surface, and make polishing paths completely cover the workpiece surface. Xu et al. [48] presented a polishing path generation method based on trochoidal tool path; they constructed a material removal model for tilted elastic pad polishing according to the position of polishing pad relative to workpiece in polishing. The uniformity of material removal along the trochoidal guide-line can be significantly achieved by optimized trochoidal step and radius, and the stability of material removal along the perpendicular direction can be effectively improved by the adaptive feed rate in simulation and experiment. The polishing quality was guaranteed. As Julien et al. [49] pointed out, tool wear and path coverage obviously affected surface properties, such as the difference in tool wear was caused by the various trochoid patterns used. Then, they proposed a method to optimize tool paths for polishing with a triangular pattern, which significantly improved the homogeneity of tool wear and the uniform of path coverage, and gained high quality surface in experiment. Pessoles et al. [50] analyzed manual polishing and then proposed a polishing path that combines the trochoidal tool path and Hilbert's curves to imitate manual polishing and reduce marks or specific patterns on the workpiece surface. Wan et al. [51] presented a novel processing form with specific path angles and steps in magnetorheological finishing, they implemented the optimal selection of the magic angle step value based on the scale-variant filtered spectrum with Fourier analysis. The experimental results shown that the selected magic angle step state can significantly suppress MSF errors. Wang et al. [52] analyzed the periodic errors on optical surface in magnetorheological jet polishing. Then, they presented Zernike extension method and the Neighbor–Gerchberg extension method, and a unicursal and partially constrained path to control the path effects. These methods can greatly diminish MSF error in simulation and experiment. Wang et al. [53] studied an optimization method for suppressing the MSF error with the tool steps, and they investigated the relationship between the tool steps and the formation of tool path ripple error through theoretical analysis and experiments. The wider the tool step size, the larger the PV and RMS values of the surface. The relationship between the tool step size and PV value of the tool path ripple error is an inverted L-shaped curve. The MSF error can

be significantly suppressed by optimizing the tool steps in the experiment.

Here are some other paths. Xie et al. [54] proposed a polishing path implementation method based on improved Prim algorithm. They analyzed the eigenvalue of the surface grid, obtained a simply connected polishing path based on the generated mesh and the distribution of dwell points. Compared with the raster path, better texture and lower MSF error were obtained in experiments. Li et al. [55] presented a novel hyper-crossing path based on wide sweeping path, which has the ability of high velocity and high acceleration in robotic polishing and can effectively suppress the MSF error.

3.1.5 Discussion on polishing path optimization

By reviewing the previous literature on polishing paths, the typically adopted polishing paths are summarized and shown in Table 2. The linear polishing path is primarily applied to the processing of planar components. Its major advantages are simple generation, high efficiency, easy realization, and low requirements for processing equipment. The spiral polishing path can be utilized to polish not only planar components, but also curved components. The pseudo random polishing path has very high requirements on the dynamic characteristics of processing equipment.

Comprehensively, when optical components need to be processed, the appropriate type of polishing path should be selected according to the surface features of the component, the processing equipment, etc. According to the process conditions and processing requirements, the path should be optimized by distribution, spacing, multi-path synthesis, and joint process parameter selection to obtain high-quality optical surfaces, which can shorten processing time, improve production efficiency, reduce equipment wear, consume less energy, etc., as shown in Fig. 9.

3.2 Optimized design of polishing tool for restraining MSF error

At present, the smoothing effect of the grinding plate is a simple and effective method among many suppression techniques, and the theoretical basis and technical approach of smoothing tool is the most mature and self-contained. This method has a good smoothing effect and low costs. Therefore, it is widely used to restrain MSF error.

3.2.1 Rigid tool

The principle of smoothing MSF error by the rigid tool is shown in Fig. 10. The high point of the optical surface will preferentially contact the rigid tool during the polishing process, and then, there is a pressure difference between

Table 2 Comparison of different polishing paths

Path	Material/shape	Tool	Polishing time	Surface quality	Author
Scanning/raster path	BK7/flat 30 mm×30 mm	Bonnet tool	—	PV = 35.9 nm RMS = 7.0 nm	Wang [38]
	BK7/flat Φ35 mm	Bonnet tool	30 min	PV = 10.29 nm RMS = 7.0 nm	Dunn [36]
Hilbert path	BK7/flat 30 mm×30 mm	Bonnet tool	—	PV = 92.6 nm RMS = 16.5 nm	Wang [38]
Maze path	BK7/flat 30 mm×30 mm	Bonnet tool	—	PV = 99.1 nm RMS = 17.1 nm	Wang [38]
Peano-like path	BK7/parabolic Φ100 mm	MRF	145 min	PV = 0.097λ RMS = 0.011λ Ra = 0.91 nm	Tam [26]
Spiral path	Fused silica/ Concave spherical Φ230 mm	AFP	—	PV = 50.268 nm RMS = 3.608 nm Rq = 0.233 nm	Liu [30]
	Nucleated glass/flat Φ90 mm	MRF	30 min	PV = 0.386λ RMS = 0.059λ	Hu [31]
	Aluminum/aspheric Φ10 mm	Polyurethane tool	—	Ra = 0.8893 μm	Qu [34]
Pseudo-random path	BK7/flat Φ35 mm	Bonnet tool	60 min	PV = 35.21 nm RMS = 5.24 nm	Dunn [36]
Part-random path	—/Flat Φ92 mm	MRF	7.46 min	PV = 0.062λ RMS = 0.010λ	Dai [37]
Hyper-crossing	Aluminum/freeform 400 mm×400 mm	Silly Putty tool	120 min	Sa = 2.9 nm	Li [55]

the high point and the low point. Thereby, the amount of residues removal at the low point is less than the amount of residues removal at the high point. Eventually, the amount of residues removal at the high point can be removed preferentially. The implementation of smoothing is based on the following two items, the rigid tool should have the proper

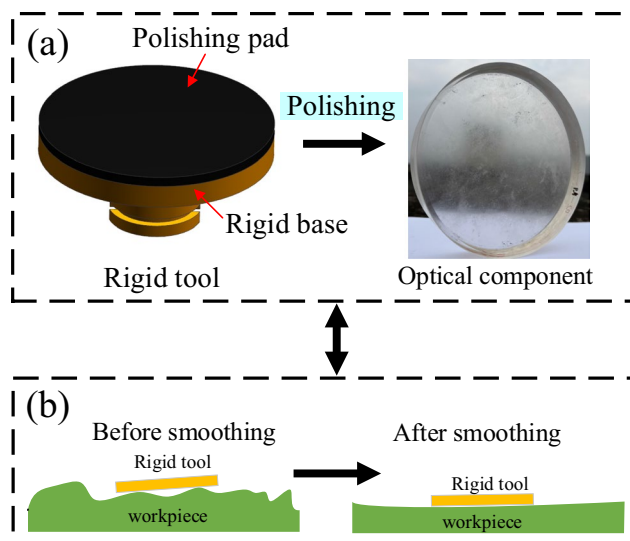**Fig. 9** Summary of polishing path optimization methods [25–54]
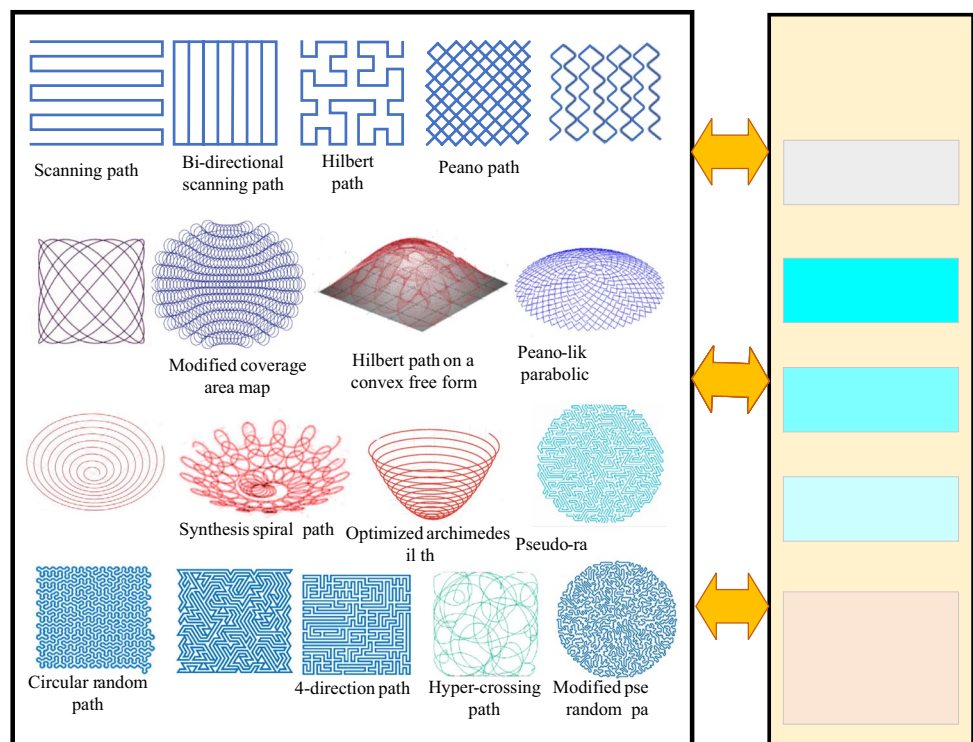
Fig. 10 Rigid tool for smoothing MSF error. **a** Component is smoothed by rigid tool and **b** smoothing principle of rigid tool

Fig. 11 Flexible tool for polishing aspheric component

stiffness and the appropriate diameter, and the diameter of the rigid tool should be able to cover the spatial period length of the error to be smoothed [56].

Some literatures have elaborated various mathematical models of the smoothing pad for smoothing. For example, Hou et al. [57] performed a quantitative analysis of the smoothing process, then extrapolated a predictable smoothing evolution model based on the pitch pad, and used the pitch pad to smooth the optical surface, so that the surface ripple error generated on the optical surface can be more accurately predicted. A smoothing evolution model with the Bridging model and Preston's equation was presented by Shu et al. [58], which is used to build the mathematical mapping relationship between the surface error and smoothing time in smoothing processing using a pitch tool. Experiments show that the model can accurately predict the smoothing effect. Yu et al. [59] analyzed the misfit between the polishing tool and the workpiece in polishing aspheric surfaces, and then designed a rigid smoothing tool to reduce the MSF error of the aspheric optical surface. They optimized the parameters of the smoothing tool according to the conic constant and tilt angle, and significantly achieved the removal of the MSF error on aspheric surface in experiment. Dong et al. [60] analyzed the contact state between the flat-pitch polisher and workpiece in the polishing by using the finite element method, and then established a numerical simulation of TIF to modify the model of the simulated TIF. They realized that the removal shape of the simulated TIF was closer to the removal shape of the actual TIF in the experiment, and can more accurately predict the actual TIF. Walker et al. [61] addressed the problem that the hard tools used for smoothing aspheric or freeform surfaces are prone to induce the MSF
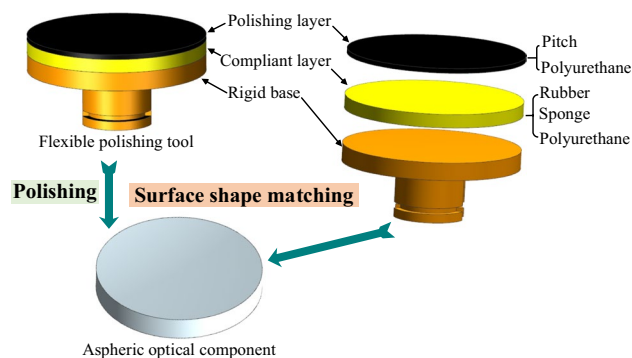
error. A novel glass-bending rig was used by them to smooth aspheric, which has the characteristics of variable complex surface shape within a continuous range and the ability to bear processing pressure. Then, they established the relationship between tool misfit, abrasive grit size, and the MSF error generated on the surface. Chen et al. [62] analyzed the posture-changing relationship between the pitch tool and the workpiece in polishing. They investigated the instability of the removal function with the local asphericity of the optical surface and the viscoelasticity of the tool through theoretical analysis and experiments.

In combination, the rigid smoothing tools are mostly applied to smooth planar components and regular spherical components. Its mathematical model is relatively simple, smoothing efficiency is high, and manufacturing cost is low.

3.2.2 Compliant polishing tool

The earliest flexible polishing tool was designed by Mehta et al. [63, 64] in 1990, They expected to use the flexible polishing tool to solve problems such as the mismatch between the rigid small grinding head and the surface shape of optical components, and the uneven force between the polishing tool and the component surface. The structure of the tool is shown in Fig. 11. They analyzed the force distribution and elastic deformation of the flexible polishing tool based on elastic mechanics, and established a bridging model for evaluating the smoothing effect of polishing tools. Nie et al. [65] considered that Mehta's bridging model can theoretically effectively describe the smoothing effect of polishing tools on the MSF and HSF errors. This classic theoretical model was difficult to deal with irregular medium and high-frequency errors in actual optical processing, so a universal numerical model was established based on the finite element analysis method. Through numerical calculation, the model can effectively predict the force distribution between the bottom of the polishing tool and the irregular MSF and HSF errors on the optical component surface during smoothing. Furthermore, a universal numerical model based on the

finite element was proposed by Nie et al. [66], who investigated the influence of the groove of the grinding pad on the smoothing of the MSF errors and established the relationship between the type, depth, and width of the grinding pad groove and the pressure distribution at the bottom of the grinding pad, as shown in Fig. 12. The optimal combination of the above parameters was obtained through the optimization algorithm. A polishing pad with optimal combination parameters was used to smooth a 100-mm diameter fused silica flat mirror. The resulting Zenik 36 residual on the mirror surface was reduced from 2.38 to 0.68 nm.

The bonnet tools with flexible inflated structure are also primarily used as ultra-precision machining tools [34, 67]. Walker et al. [68] designed a machining tool, which is a bonnet with the characteristics of inflated, bulged, and the surface covered with non-pitch flexible material. Variable spot-size and dynamic control were achieved. Flat, spherical, and aspherical surfaces can be polished and figured by using the tool. Wang et al. [69] analyzed the contact posture between the bonnet tool and the workpiece in polishing. The force of the bonnet tool and the workpiece contact area was analyzed by using the finite element method. Then, they established the mathematical model and geometric model of the static tool influence function for bonnet polishing with tilted polishing, discrete precession polishing, and continuous precession polishing, respectively. A prediction model of the tool influence functions of the bonnet tool was developed by Li et al. [70, 71], and they realized the optimization of polishing multiple parameters and investigated the pressure distribution between the polishing tool and the workpiece in polishing by finite element analysis. The accuracy of the model has been demonstrated experimentally. A co-processing method combining the atmospheric pressure plasma machining method with the bonnet polishing method was adopted by Su et al. [72] for the ultra-precision machining of optical components. Then, a combined processing chain was established. They used the bonnet tool to smooth out the residual error produced by atmospheric pressure plasma
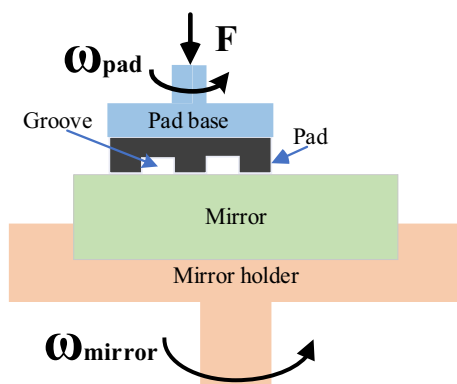
processing. This combined processing method have been experimentally proven to be very effective and efficient. Pan et al. [73] analyzed the movement mechanism of the bonnet tool in polishing, and then established a sub-steps precession model for bonnet polishing, which is used to optimize the conformal polishing process. The model have significant effect, which is validated by simulation and experiment. Wang et al. [74] optimized the major parameters of bonnet polishing (polishing pressure, z offset, polishing path spacing, bonnet tool speed, and bonnet tool tilt angle) based on the minimum residual error method. The order of importance of the influence of these parameters on the residual error was obtained.

Some other flexible processing tools are also used to polish. There is a new fiber-based tool designed by Shahinian et al. [75–77], who used the glued cylindrical bars with twelve fibers to reduce the MSF errors of the optical surface in processing. The characteristics of the tool is that it can maintain its shape stably and keep the material removal profile consistent during machining. They have analyzed the movement state between the tool and the workpiece edge by finite element modeling and experimental testing. The tool has a significant effect on reducing the pre-existing MSF error of optical component surface by using raster path polishing, which has been demonstrated in experiments.

3.2.3 Semi-flexible polishing tool

Michael et al. [78] analyzed the relationship between the stiffness of the grinding pad and the ability to remove the MSF error using the Fourier expansion method based on the research of Pravin et al. Furthermore, they established a mathematical model between the structural stiffness at the bottom of the grinding pad and the specific error frequency of the optical component surface, which shows that the smoothing process of the mill pad for the MSF and HSF errors is a selective filtering process for the specific frequency errors. For aspheric surface, the deviation of its contour from that of the spherical surface is a low frequency error. The smooth grinding pad should be designed to maintain the low frequency profile of aspheric surface and selectively remove the mid-to-high spatial frequency errors that affect the energy of the optical system. Therefore, Michael et al. proposed to use a semi-flexible tool with sandwich structure to smooth the MSF error of aspheric surface. The semi-flexible tool is composed of a rigid substrate, a deformation layer, a metal sheet, and a polishing layer. This special sandwich structure enables the pad to have the ability of high-pass filter in smoothing, as shown in Fig. 13. So, it can effectively remove the MSF error.

Wang et al. [79] designed a semirigid bonnet with high efficiency and certainty in optical polishing. The tool includes a metal sheet, a rubber membrane, and a polishing

Fig. 12 The grooved polishing pad is in contact with the mirror [66]

Fig. 13 Semi-flexible polishing tool [78]
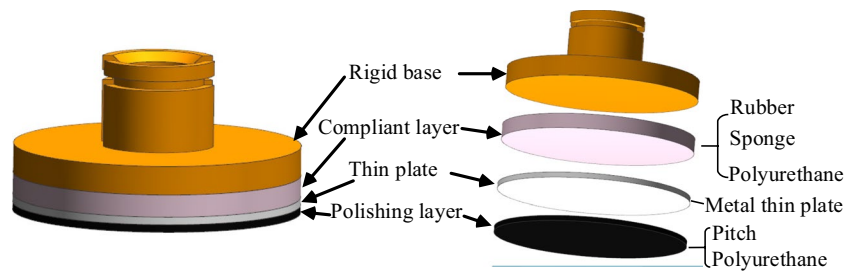
pad, which provides a higher degree of stiffness than a normal bonnet tool. The MSF error was highly depressed by the tool, and the high-precision surface was achieved in experiment.

The rigidity of polishing tools significantly affects the polishing quality of aspherical components. Its excessive rigidity makes the consistency between the tool surface and the aspherical component surface very weak, and makes it difficult to polish the non-contact area between the tool and the component. Its stiffness is too small. Although the surface of the polishing tool can conform to the surface of the aspherical component, the error on the aspherical surface is difficult to be eliminated. There is a rigidity controllable polishing tool proposed by Wang et al. [80], as shown in Fig. 14. They designed a rigidity controllable mechanical structure based on magnetorheological elastomers for smoothing aspherical surfaces. It consists mainly of a thin

plate, a rigid layer, a magnetorheological elastomers layer with chain-like structure, and a polishing layer, which can significantly reduce the MSF error.

Subsequently, Li et al. [81] analyzed a multi-layer polishing tool and presented a mathematical model based on the deformation of the multi-layer polishing tool in smoothing, as shown in Fig. 15. It can calculate the pressure distributions, the compression, bending, and the shearing deformation between the polishing tool and the workpiece accorded to Galerkin's displacement functions. The validity of the model was demonstrated by comparing the rigid tool with the semi-flexible tool in simulation and experiment.

In the above description, the semi-flexible polishing tools are designed to smooth the mid-to-high spatial frequency errors in aspheric surface processing. Therefore, the anastomosis between the smooth grinding pad and the local area of the aspheric surface can be improved by reducing the

Fig. 14 Rigidity controllable polishing tool [80]. **a** 3D model, **b** schematic diagram, and **c** actual hardware
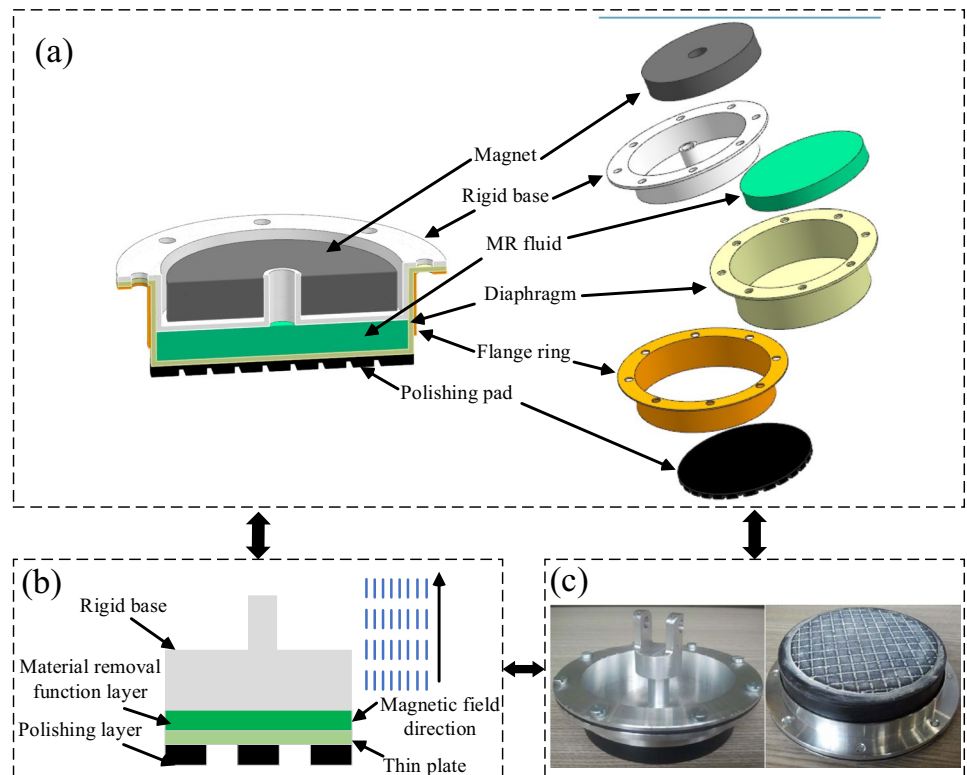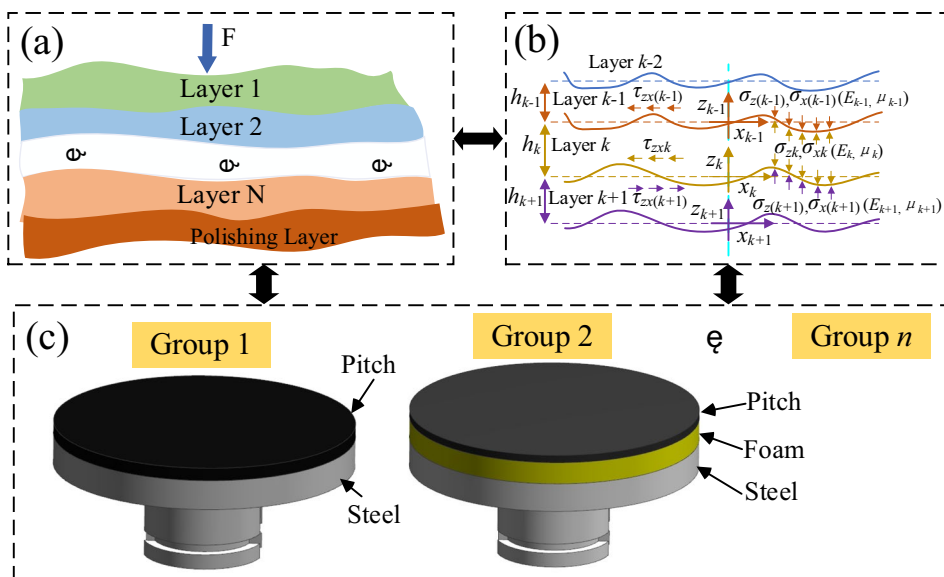
Fig. 15 Multi-layer polishing tool in the smoothing process [81]. **a** Schematic diagram of multi-layer tool, **b** coordinate systems, and **c** 3D Structure of polishing tools in different groups

diameter of the grinding pad. The mid-to-high spatial frequency errors of the flat or spherical surface can be easily suppressed by processing with the traditional flat or spherical integral pad to obtain surface roughness better than 0.4 nm. However, the semi-flexible polishing tool is not suitable for machining large off-axis offsets aspheric surface. Its surface curvature variation range is narrow, which is difficult to match the variation range of large off-axis offsets aspheric surface curvature.

3.2.4 Conformal polishing tool

The Vibe method of high-frequency vibration polishing was proposed by Jessica et al. [82] to remove mid-to-high spatial frequency errors in polishing aspheric surfaces, as shown in Fig. 16. In this method, the full-aperture polishing pad is used to anastomose 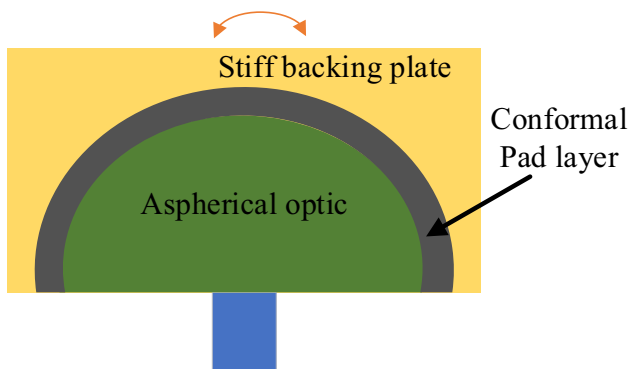over aspheric optics and smooth out the mid-to-high spatial frequency errors. The polishing pad with high stiffness can generate high-frequency random vibration in a small scale.

There is a new conformal vibration polishing method presented by Liu et al. [83] to reduce the MSF error. The method focused on movement regularity, contact relationship, material removal characteristics, and accurate prediction of smooth machining based on the time-domain smoothing model. Theoretical and experimental results show that the method has high material removal efficiency and remarkable smoothing effect. Hou et al. [84] proposed a short-stroke forced vibration polishing technology based on full-aperture conformal vibration polishing, and investigated in depth the processing mechanism and material removal characteristics of the method. The MSF errors of optical surface can be uniformly smoothed out, and the original surface shape can be stably maintained in experiments. Zhang et al. [85] designed a new vibration-assisted conformal polishing tool, which they used to reduce surface roughness and obtain high-quality parts in experiment. Dieste et al. [86] presented a new conformal polishing method based on tool footprints, and accurately predicted the total amount of material removal in polishing through the established mathematical model. There is a conformal smoothing means with ultra-precision continuous phase plates established by Song et al. [87]. They used the finite element method to analyze the polishing force distribution. The optimization of the smoothing process parameters was achieved, and the MSF error was effectively reduced.

Vibe is a full aperture coverage polishing technique that can be used to polish optical surfaces with various shapes, for example, conformal optical surfaces, freeform surfaces, deep convex, and deep concave shapes, which are difficult

Fig. 16 The VIBE polishing processing [82]

to process with other optical polishing technologies. The Vibe conformal machining method has a high processing efficiency. It can be used to quickly remove material in the pre-polishing stage, and also can remove sub-surface damage of the optical components in the initial polishing stage. Compared with the traditional polishing method, its removal efficiency is increased by 10–50 times. The Vibe method also can smooth out mid-to-high spatial frequency errors on the optical surface by reasonably selecting vibration frequency, polishing pressure, and conformal flexible layer materials [88–92].

3.2.5 Rigid conformal polishing tool

The successful application of computer-controlled surface shaping (CCOS) relies on a stable and deterministic removal function. The dwell time of the removal function at different positions on the optical component surface is controllable. By controlling the dwell time, CCOS can achieve a defined amount of material removal profile. For physical contact polishing, it is necessary to have a close and stable contact between the optical component surface and the polishing pad to ensure the stability of the removal function. In view of the above, Kim et al. [93] structured a rigid conformal (RC) polishing tool and designed the parametric smoothing model. The model is based primarily on the periodic sine and cosine mid-to-high spatial frequency error theory and is an ideal model. The structure of the RC is shown in Fig. 17. The flexible support layer of the RC polishing tool is made of Silly-Putty (plasticine), which is a non-Newtonian fluid material and is essentially a viscoelastic material. The plasticine is sufficient fluid to deformed to match the aspheric surface in real time during processing. Moreover, plasticine also has a large elastic modulus under high-speed impact. Therefore, plasticine can also strongly smooth out the MSF error.

Further, Su [94] proposed a correlation smoothing model based on the parametric smoothing model that expands the ability to perform quantitative smoothing using general surface data with complex irregularity. Song et al. [95] desigigid conformal polishing tool with a new structure, which

Fig. 17 3D schematic RC lap structure [93]

has a highly stable and approximate theoretical TIF to overcome the extreme polishing prned a new ressure of the time-dependent smoothing evacuation model. The MSF error was almost fully smoothed out in a series of experiments.

3.2.6 Comparison of different tools

In the above, we have detailed four types of polishing tools, including rigid polishing tools, semi-flexible tools, compliant tools, and rigid conformal polishing tools. The simplified structure of these four tools is shown in Fig. 18. Table 3 shows the comparison of different polishing tools. Their respective characteristics are summarized as follows.

Rigid tool (such as pitch tools) is the most widely and commonly used polishing tool for polishing flat and spherical workpieces. The tool is traditionally structured with a solid base pad and a polishing material with pitch or polyurethane. The rigid tool has good smoothing effect, high smoothing efficiency, and low manufacturing cost. However, for polishing spherical workpieces, different spherical workpieces need to be matched with rigid tools with the corresponding curvature radius, so the rigid tools are less versatile. Moreover, they are hardly maintainable.

Semi-flexible tool is mainly applied to polish flat, spherical, and aspheric workpieces, which can efficiently smooth the MSF error. The tool consists of a rigid layer with a solid base pad, a compliant layer, a thin layer, and a polishing layer. The working principle of the tool is similar to a high-pass filter, which can smooth out the MSF error without damaging the surface figure. It can be applied to workpieces with different low-order curvature. It is easy to repair. However, its smoothing efficiency is lower than that of rigid tool and its manufacturing cost is relatively high.

Compliant tool can be adopted to polish workpieces with various curved surfaces, including flat, spherical, aspherical, and freeform surfaces. The tool is basically built with a solid base pad, a compliant material with liquid or air in a container, and a polishing layer. It can be applied to process all types of surface-shaped optical components and has good versatility, but its smoothing efficiency is low, the smoothing effect is weak, and the manufacturing cost is high.

Rigid conformal polishing tool can also be used to smooth optical components with various curved surfaces. The tool includes a solid base pad, a cavity container containing non-Newtonian fluid, and a polishing layer. Its smoothing effect is satisfactory, and the smoothing efficiency is higher than that of the compliant tool and the semi-flexible tool, respectively. However, its processing range is limited, and it is difficult to be used for optical components with large curvature changes. Additionally, it is easy to maintain.

Depending on the characteristics of the optical components to be processed, such as surface shape, curvature changes, machining accuracy, processing time, and other
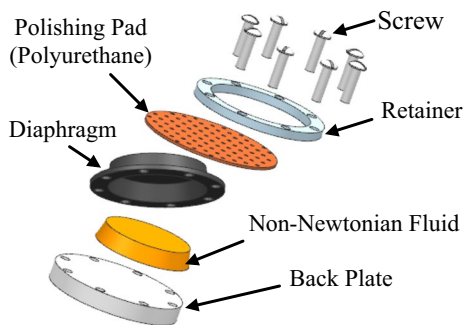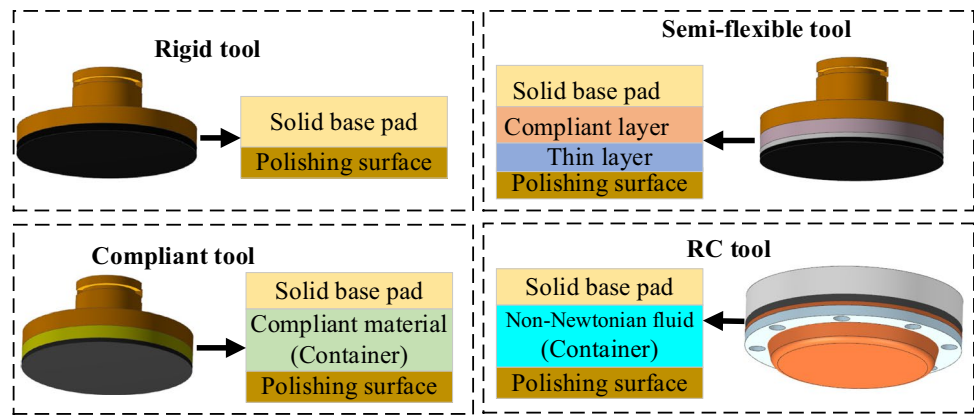
Fig. 18 Comparison of four polishing tools with different structures

factors, the appropriate polishing tools are selected for smoothing to obtain high-quality optical components with high efficiency and low cost.

3.3 Ion beam sacrifice layer for removing MSF error

Ion beam sacrifice layer polishing technology is implemented to remove mid-to-high spatial frequency errors. First, a sacrificial layer is formed which can be uniformly removed, and this sacrificial layer can be covered with a thin film over the optical component surface by some special means. The uneven surface is covered by the sacrificial layer, which makes the uneven surface smooth. Then, the optical surface is polished using the ion beam polishing technology. The coating is uniformly removed together with the uneven optical surface material to achieve a smooth optical surface [96, 97]. Its technical principle is shown in Fig. 19. The ion beam sacrificial layer polishing technology can effectively suppress the mid-to-high spatial frequency errors without destroying the original surface shape accuracy. Because of the low requirements for the uniformity of photoresist, it can be applied to the processing of mid-to-high spatial frequency errors of planar, spherical, aspherical, and freeform surfaces [98–100].

3.4 Some other technologies for removing MSF error on optical surfaces

Among ultra-precision polishing methods, there are also some non-contact polishing techniques, which are largely

adopted for smaller scale processing. It mainly includes elastic emission polishing processing method [101, 102], nanoparticle colloid jet polishing method [103], float processing method [104, 105], microjet processing method [106, 107], and other methods. These methods are all based on hydrodynamic for polishing [108], which can achieve small amount of material removal and high processing accuracy, and obtain high-quality optical components with minimal surface roughness, minimal surface or sub-surface damage, crystal surface with complete crystal structure, and minimal surface residual stress. However, these methods have weak ability to restrain the MSF error, and also have shortcomings such as low material removal rate, unstable material removal rate, low processing efficiency, and difficulty in using for mass production.

4 Discussions

According to the above literature and related analysis, the technical characteristics of several commonly used smoothing methods are shown in Table 4. Table 4 shows the advantages and disadvantages of each method. Each method has its own specific application scenario and is applied in its scenario respectively.

Generally, the polishing path optimization method is preferred for processing to improve the local surface quality of optical components, provided that the existing processing equipment remains unchanged. This is achieved by selecting

Table 3 Comparison of different polishing tools

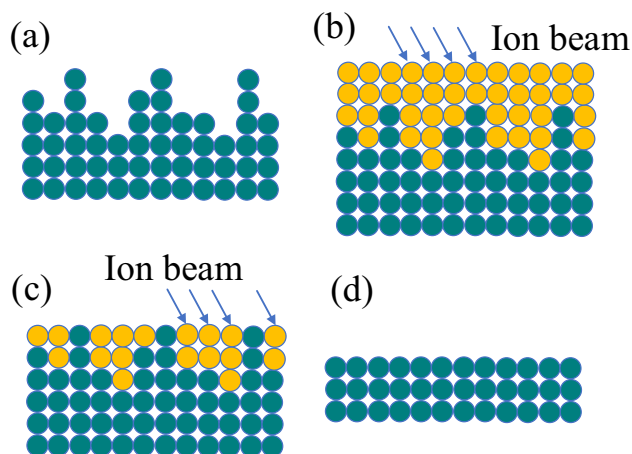| Tool	Removal rate	Smoothing effective	Shape applicability	Maintainability	Subsurface damage	Cost	Reference
Rigid tool	High	Excellent	Poor	Poor	Yes	Low	[56–62]
Flexible tool	Low	Poor	Good	Good	No	High	[63–74]
Semi-flexible tool	Medium	Good	Medium	Good	No	Medium	[78–81]
RC tool	Medium	Good	Medium	Good	No	High	[93–95]

Fig. 19 Schematic diagram of the ion beam sacrifice layer method. **a** The original surface topography, **b** covering sacrificial layer and polishing, **c** polished to substrate, and **d** after the sacrificial layer is completely removed

the best path type, reasonable path distribution, optimal path spacing, edge removal optimization, etc. The path optimization method is cheap to manufacture but suffers from the limitations of processing equipment. Uneven material removal and surface ripple errors caused by the processing path can only be minimized by optimizing the processing path. Using polishing path optimization method, there are significant manufacturing limits to the accuracy of existing component manufacturing and it is difficult to achieve higher scale accuracy.

For the optimal design of polishing tool method, it is mainly used in the following situations: First is that the machined surface of the polishing tool does not match the surface of the component; the surface of the tool is difficult to conform to the surface of the component being machined. This requires the structure of the polishing tool to be redesigned and optimized. Second, the removal function of existing polishing tools is unstable. The polishing tool are deformed greatly and worn seriously during processing,

resulting in unstable removal function. It is necessary to select new structures and new materials to enhance the stability of its structure and maintain a stable removal function. Third, the rigidity of polishing tools is difficult to adapt to the machining of the required components, especially for aspherical and free-form components. If the rigidity of the tool is too large, the processing surface of the tool is difficult to be conformed to the surface of component. If the rigidity of the tool is too low, the material removal rate of the component is low or the material on the component is difficult to removed. This requires redesigning the tool structure or rebuilding the tool with new materials to produce a tool with the adequate stiffness to complete the machining of the workpiece. The ion beam sacrifice layer smoothing method is primarily applied to ultra-smooth surface processing. It corrects for small errors on the component surface to improve the accuracy scale.

To improve the manufacturing accuracy of optical components, it tends to be processed by an integrated method, as shown in Fig. 20. The MSF error suppression technology is an integrated processing technology. The polishing path must be generated according to the corresponding polishing tool and polishing method during processing. Each polishing tool will preferentially select the corresponding optimal polishing path that matches it for optical processing. The traversal of the polishing path and the movement control of the polishing tool must rely on intelligent control system.

Magnetorheological finishing, ion beam figuring, bonnet polishing, etc., are currently widely adopted for optical processing. These modern processing technologies are used to deterministically reduce the surface errors in the local area of the optical components by small-scale removal function. The polishing process will inevitably generate ripple errors equivalent to the scale of the removal function. According to the processing principle of the sub-aperture processing technology, some frequency errors can be corrected to a certain extent by reducing the size of the removal function, controlling the tool path distance and improving the positioning accuracy of machine tool. However, as the size of the

Table 4 Comparison of different restraining MSF technologies

Technologies	Peculiarity
Polishing path Optimization method	Relying on various path planning algorithms, the advantage is the high efficiency of process preparation. While the disadvantage is that it is difficult to implement for complex algorithms, it requires high positioning accuracy and fast response speed for the equipment
Optimal design of polishing tool method	Smoothing by designing various polishing tools has the advantages of extensive research foundation, mature theory, low requirements for equipment accuracy, high smoothing efficiency, etc. The disadvantage is that a single polishing tool can only be used for specific component processing and its versatility is limited
Ion beam sacrifice layer smoothing method	The advantages are high smoothing accuracy, which can be used for processing various surface components. While the disadvantages are difficult to determine the sacrificial layer material, complex process, low smoothing efficiency, and high cost

Fig. 20 Summary diagram of MSF suppression technologies for optical polishing
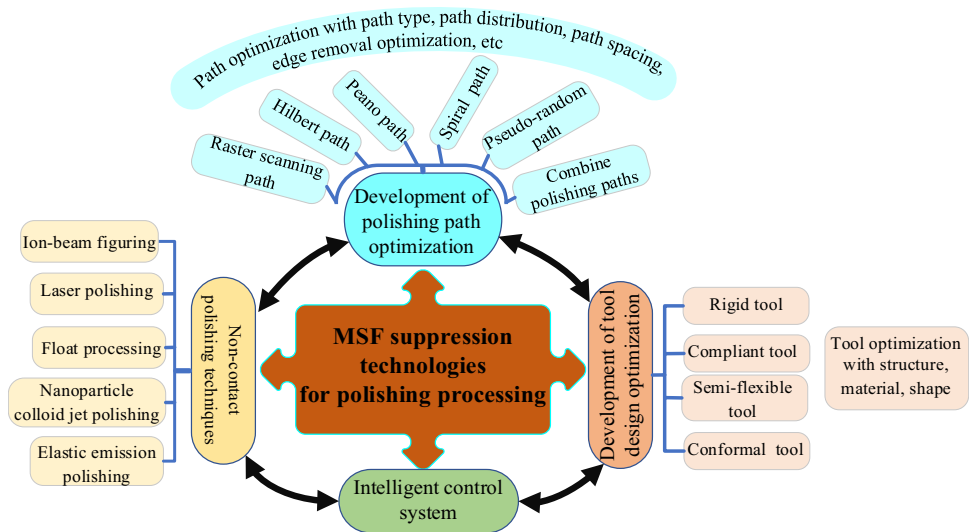
removal function decreases, the removal efficiency declines greatly. Seriously, the smaller the size of the removal function, the more easily the optical machined surface is fragmented. This is not significantly effective in improving the MSF error. The idea of using a small size removal function to correct the MSF error is also limited by the positioning accuracy of the machine tool.

Reviewing the current state of research on MSF error suppression technologies. The current literature focuses on sub-aperture tool smoothing, full-aperture tool smoothing, trajectory randomization to average non-periodic error, etc. These are traditional contact polishing methods. These methods finally achieve high accuracy optical components by smoothing the mid-to-high spatial frequency errors, which are difficult to break through the precision level. Combining traditional smoothing tools and contact machining methods to suppress the MSF error has significant limitations. First of all, the basic material removal principle of the contact tool processing is the same as that of CCOS processing. The polishing abrasive is pressed into the optical component surface by normal polishing pressure, and then micro-fragments are removal from the optical component surface by the rotation and movement of the polishing tool. The material removal mechanism determines that there are tiny scratches on the optical surface, and even some destruction layers with a certain depth on the micro-scale of the optical surface, due to the processing with the contact tool. Secondly, the principle of the flexible tool for smoothing the MSF error on the aspheric surface is based on the passive deformation of the flexible tool to achieve the coincidence with the low-frequency surface contour of the aspheric surface, whose surface deviation deformation shows a strong stiffness. Thereby, the MSF error can be effectively smoothing out. The processing principle shows that the force on the flexible polishing tool is uneven during smoothing. There

is a pressure difference between the high point and low point of the aspheric contour, which leads to the generation of new MSF error. Meanwhile, the flexible polishing tool is adopted to processing aspheric surfaces, the amount of material removal is always changing due to the continuous change in the contact state between the bottom of the tool and the aspherical surface. Therefore, this will also make the flexible polishing tool introduce new MSF error in polishing.

In summary, conventional contact tools for smoothing optical surface have a number of inherent shortcomings and face serious challenges when machining high-precision optical components, such as high-precision components required for extreme optical development projects such as synchrotron radiation optics and nanolithography. The mid-to-high frequency errors at the deep sub-nanometer level on the surface of these optical components should be suppressed. Therefore, it is urgent to develop and research new MSF error suppression technology, and further improve the accuracy of optical components based on the traditional MSF error suppression technology.

5 Summary and prospect

In this paper, several widely adopted suppression technologies of the MSF error in optical processing are reviewed, focusing on polishing path optimization method, polishing tool structure optimization method, conformal polishing method, and ion beam layer removal method. The principles, characteristics, and development process of each are introduced in detail; then, their advantages and disadvantages are compared.

In the future, there are four promising directions of MSF error suppression technology in optical processing.

One direction is further to study the key technologies of complex surface polishing. By refining the theoretical geometric model of complex surface components, exploring mathematical expressions, designing a dynamic optimization polishing path algorithm, establishing the variable curvature removal function model of the surface and the real-time polishing compensation algorithm, and adopting a dynamic dwell time model to further reduce the error caused by the polishing path. Open intelligent polishing system will be widely applied to optical processing, which combines artificial neural networks, fuzzy control, genetic algorithm, expert systems, and other advanced artificial intelligence techniques and modern control methods. Advanced technologies such as artificial neural network are used to obtain the real surface features of optical components by recognizing the data sensed by multiple input sensors. The appropriate polishing process is deduced by expert knowledge, and the global optimal solution of polishing model is produced by intelligent optimization algorithms, which will ultimately make the polishing system have learning ability, reasoning ability, and sufficient self-adaptation ability.

The second direction Is adopted to address big data. Optical processing is developing towards intelligent manufacturing, which includes real-time, online, and rapid inspection of the surface topography of processed optical components, intelligent optimization of polishing paths, intelligent optimization of polishing process parameters, intelligent optimization of the polishing process, etc. Optical high-precision manufacturing will integrate the cross-integrated knowledge of multiple disciplines such as physics, advanced manufacturing, precision machinery, intelligent control, computer technology, information perception and processing, intelligent algorithms, and big data and other disciplines, and integrate mechanical optimization, intelligent detection, precision mechanical design, intelligent control, etc. Intelligent deterministic removal of surface materials of complex curved optical components is constantly realized, and the generation of error is continuously reduced, which further realizes the high precision, high efficiency, and low cost manufacturing of optical components.

The third direction is the development of new machining tools, which includes the application of new materials for processing tools and the designing of new structures for machining tools. It is critical to develop polishing tools that can closely conform to the complex shape of optical surfaces and maintain their stable removal function to achieve the deterministic removal of materials of complex curved surfaces. A prediction model for process parameters related to surface roughness and material removal efficiency will be established to predict surface roughness and material removal efficiency based on real-time dynamic machining states. Combined big data analysis and deep learning, a real-time compensation algorithm for the material removal model will be established. The manufacturing process of ultra-precision optical components will be intelligently controlled. Those machining tools will be integrated with the computer integrated manufacturing system for processing high-precise or ultra-precise optical components.

The fourth direction is the development of some flexible and non-contact processing methods, such as elastic emission machining processing, micro-fluidization processing, and nanocolloidal particle jet polishing processing. These technologies can control the MSF error of the optical component surface to better than 0.3 nm (RMS), and significantly reduce micro-scale fragment scratches, sub-surface damage layers, and sub-surface stress damage on the processed surface. There is an urgent need to further explore these emerging processing technologies, which are currently being investigated for material removal mechanisms mainly through experiments and simulations. These techniques have no specific chemical or physical principles or mathematical model formulas for the material removal mechanism at the atomic level. As a result, there are currently serious weaknesses in the application of these techniques to processing. This brings certain difficulties to the application of these processing techniques. It is necessary to further combine the knowledge of elasticity, molecular dynamics, and quantum mechanics to accurately describe the interaction processes between the polishing medium and optical components, to further establish the theoretical foundation, and to investigate how these technologies can be applied to the processing of large-diameter optical components. Therefore, the application of these technologies to improve the manufacturing efficiency is an important development direction in improving the surface quality of optical components and in manufacturing large diameter optical components.

Code availability Not applicable.

Declarations

Ethics approval Not applicable.

Consent to participate Not applicable.

Consent for publication Not applicable.

Conflict of interest The authors declare no competing interests.

References

1. Krishnan A, Fang F (2019) Review on mechanism and process of surface polishing using lasers. Front Mech Eng 14:299–319
2. Peng Y, Shen B, Wang Z, Yang P, Yang W, Bi G (2021) Review on polishing technology of small-scale aspheric optics. Int J Adv Manuf Technol 115:965–987
3. Xia Z, Fang F, Ahearne E, Tao M (2020) Advances in polishing of optical freeform surfaces: a review. J Mater Process Technol 286:116828
4. Lu Y, Xie X, Zhou L (2016) Design and performance analysis of an ultraprecision ion beam polishing tool. Appl Opt 55:1544–1550
5. Jiang R, Li M, Yao Y, Guan J, Lu H (2019) Application of BIB polishing technology in cross-section preparation of porous, layered and powder materials: a review. Front Mater Sci 13:107–125
6. Kasai T, Harvey JE, Thompson AK (1995) Scattering effects from residual optical fabrication errors. SPIE 2576:155–174
7. Shu Q, Hai K, Huang W, Jiang L, Yuan S, Li K, Sun P, Tian D, Zhang Y (2022) Evolution law of comet-shaped defects in magnetorheological finishing. Appl Opt 61:691–698
8. Preston F (1927) The theory and design of plate glass polishing machines. J Soc Glas Technol 11:214–256
9. Liao D, Yuan Z, Tang C, Xie R, Chen X (2013) Mid-spatial frequency error (PSD-2) of optics induced during CCOS and full-aperture polishing. J Eur Opt Soc Rap Publ 8:1–5
10. Pan JW, Chu J, Zhuang S, Yao YS, Jiang B, Ma Z (2017) Li QX (2018) Edge effect modeling of small tool polishing in planetary movement. Young Sci Forum 10710:1–10
11. Satake U, Enomoto T, Miyagawa T, Ohsumi T, Nakagawa H, Funabashi K (2019) Achieving stable removal rate in polishing with small tools. Precis Eng 55:248–253
12. Satake U, Enomoto T, Miyagawa T, Ohsumi T, Nakagawa H, Funabashi K (2019) Stabilization of removal rate in small tool polishing of glass lenses. Int J Autom Technol 13:221–229
13. Kim SH, Nam E, Ha TI, Hwang SH, Lee JH, Park SH, Min BK (2019) Robotic machining: a review of recent progress. Int J Precis Eng Manuf 20:1629–1642
14. Wang QH, Liang YJ, Xu CY, Li JR, Zhou XF (2019) Generation of material removal map for freeform surface polishing with tilted polishing disk. Int J Adv Manuf Technol 102:4213–4226
15. Feng M, Wu Y, Wang Y, Zeng J, Bitoh T, Nomura M, Fujii T (2020) Effect of the components of magnetic compound fluid (MCF) slurry on polishing characteristics in aspheric-surface finishing with the doughnut-shaped MCF tool. Precis Eng 65:216–229
16. Gu Y, Kang M, Lin J, Liu A, Fu B, Wan P (2021) Non-resonant vibration-assisted magnetorheological finishing. Precis Eng 71:263–281
17. Guo Y, Yin S, Ohmori H, Li M, Chen F, Huang S (2022) A novel high efficiency magnetorheological polishing process excited by Halbach array magnetic field. Precis Eng 74:175–185
18. Nie M, Cao J, Li J, Fu M (2019) Magnet arrangements in a magnetic field generator for magnetorheological finishing. Int J Mech Sci 161–162:105018–105026
19. Paswan SK, Singh AK (2019) Analysis of surface finishing mechanism in a newly developed rotational magnetorheological honing process for its productivity improvement. Wear 426–427:68–82
20. Arnold T, Pietag F (2015) Ion beam figuring machine for ultraprecision silicon spheres correction. Precis Eng 41:119–125
21. Chernyshev A, Chkhalo N, Malyshev I, Mikhailenko M, Pestov A, Pleshkov R, Smertin R, Svechnikov M, Toropov M (2021) Matrix based algorithm for ion-beam figuring of optical elements. Precis Eng 69:29–35
22. Ding JT, Fan XW, Xu L, Ma Z, Wang YJ, Wu XG (2020) High-precision resin layer polishing of carbon fiber mirror based on optimized ion beam figuring process. Optik 206:163575–163583
23. Wang Y, Dai Y, Hu H, Du C, Bao J (2022) Study on rapid convergence strategy of nano-precision optical surface by ion beam figuring. Opt Commun 507:127614–127622
24. Xu M, Dai Y, Xie X, Zhou L, Li S, Peng W (2017) Ion beam figuring of continuous phase plates based on the frequency filtering process. Front Mech Eng 12:110–115
25. Tam HY, Cheng H (2010) An investigation of the effects of the tool path on the removal of material in polishing. J Mater Process Technol 210:807–818
26. Tam HY, Cheng H, Dong Z (2013) Peano-like paths for sub-aperture polishing of optical aspherical surfaces. Appl Opt 52:3624–3636
27. Hauth S, Linsen L (2010) Double-spiral tool path in configuration space. Int J Adv Manuf Technol 54:1011–1022
28. Hauth S, Linsen L (2011) Cycloids for polishing along double-spiral toolpaths in configuration space. Int J Adv Manuf Technol 60:343–356
29. Feng Y, Cheng H, Wang T, Dong Z, Tam HY (2014) Optimal strategy for fabrication of large aperture aspheric surfaces. Appl Opt 53:147–155
30. Liu J, Wang S, Zhang C, Zhang L, Chen H (2015) Path planning and parameter optimization of uniform removal in active feed polishing. Opt Eng 54:0651011–0651018
31. Hu H, Dai Y, Peng X (2010) Restraint of tool path ripple based on surface error distribution and process parameters in deterministic finishing. Opt Express 18:22973–22981
32. Han Y, Zhang L, Guo M, Fan C, Liang F (2017) Tool paths generation strategy for polishing of freeform surface with physically uniform coverage. Int J Adv Manuf Technol 95:2125–2144
33. Zhang L, Han Y, Fan C, Tang Y, Song X (2017) Polishing path planning for physically uniform overlap of polishing ribbons on freeform surface. Int J Adv Manuf Technol 92:4525–4541
34. Zhao Q, Zhang L, Han Y, Fan C (2019) Polishing path generation for physical uniform coverage of the aspheric surface based on the Archimedes spiral in bonnet polishing. Proc Inst Mech Eng B J Eng Manuf 233:2251–2263
35. Qu X, Liu Q, Wang H, Liu H, Sun H (2022) A spiral path generation method for achieving uniform material removal depth in aspheric surface polishing. Int J Adv Manuf Technol 119:3247–3263
36. Dunn CR, Walker DD (2008) Pseudo-random tool paths for CNC sub-aperture polishing and other applications. Opt Express 16:18942–18949
37. Dai Y, Shi F, Peng X, Li S (2009) Restraint of mid-spatial frequency error in magneto-rheological finishing (MRF) process by maximum entropy method. Sci China Ser E Technol Sci 52:3092–3097
38. Wang C, Wang Z, Xu Q (2015) Unicursal random maze tool path for computer-controlled optical surfacing. Appl Opt 54:10128–10136
39. Takizawa K, Beaucamp A (2017) Comparison of tool feed influence in CNC polishing between a novel circular-random path and other pseudo-random paths. Opt Express 25:22411–22424
40. Zhao Q, Zhang L, Fan C (2019) Six-directional pseudorandom consecutive unicursal polishing path for suppressing mid-spatial frequency error and realizing consecutive uniform coverage. Appl Opt 58:8529–8541
41. Zha J, Zhang H, Li Y, Chen Y (2020) Pseudo-random path generation algorithms and strategies for the surface quality improvement of optical aspherical components. Materials (Basel) 13:1–14

42. Li H, Li X, Wan S, Wei C, Shao J (2021) High-efficiency smooth pseudo-random path planning for restraining the path ripple of robotic polishing. Appl Opt 60:7732–7739

43. Beaucamp A, Takizawa K, Han Y, Zhu W (2021) Reduction of mid-spatial frequency errors on aspheric and freeform optics by circular-random path polishing. Opt Express 29:29802–29812

44. Wan S, Wei C, Hong Z, Shao J (2020) Modeling and analysis of the mid-spatial- frequency error characteristics and generation mechanism in sub-aperture optical polishing. Opt Express 28:8959–8973

45. Han Y, Zhang L, Fan C, Zhu W, Beaucamp A (2018) Theoretical study of path adaptability based on surface form error distribution in fluid jet polishing. Appl Sci 8:1–21

46. Khakpour H, Birglen L, Tahan SA (2014) Uniform scanning path generation for abrasive waterjet polishing of free-form surfaces modeled by triangulated meshes. Int J Adv Manuf Technol 77:1167–1176

47. Rososhansky M, Xi F (2011) Coverage based tool-path planning for automated polishing using contact mechanics theory. J Manuf Syst 30:144–153

48. Xu CY, Li JR, Liang YJ, Wang QH, Zhou XF (2019) Trochoidal toolpath for the pad-polishing of freeform surfaces with global control of material removal distribution. J Manuf Syst 51:1–16

49. Chaves-Jacob J, Linares JM, Sprauel JM (2013) Improving tool wear and surface covering in polishing via toolpath optimization. J Mater Process Technol 213:1661–1668

50. Pessoles X, Tournier C (2009) Automatic polishing process of plastic injection molds on a 5-axis milling center. J Mater Process Technol 209:3665–3673

51. Wan S, Wei C, Hu C, Situ G, Shao Y, Shao J (2021) Novel magic angle-step state and mechanism for restraining the path ripple of magnetorheological finishing. Int J Mach Tools Manuf 161:1–10

52. Wang T, Cheng H, Zhang W, Yang H, Wu W (2016) Restraint of path effect on optical surface in magnetorheological jet polishing. Appl Opt 55:935–942

53. Wang C, Yang W, Ye S, Wang Z, Yang P, Peng Y, Guo Y, Xu Q (2014) Restraint of tool path ripple based on the optimization of tool step size for sub-aperture deterministic polishing. Int J Adv Manuf Technol 75:1431–1438

54. Xie Y, Yang J, Huang W, Li J (2022) A tool-path planning method used in computer controlled optical surfacing based on improved prim algorithm. Int J Adv Manuf Technol 119:5917–5927

55. Li H, Walker DD, Zheng X, Su X, Wu L, Reynolds C, Yu G, Li T, Zhang P (2019) Mid-spatial frequency removal on aluminum free-form mirror. Opt Express 27:24885–24899

56. Kim DW, Park WH, An HK, Burge JH (2010) Parametric smoothing model for visco-elastic polishing tools. Opt Express 18:22515–22526

57. Hou J, Lei P, Liu S, Chen X, Wang J, Deng W, Zhong B (2020) A predictable smoothing evolution model for computer-controlled polishing. J Eur Opt Soc Rapid Publ 16:1–11

58. Shu Y, Nie X, Shi F, Li S (2014) Smoothing evolution model for computer controlled optical surfacing. J Opt Technol 81:164–167

59. Yu G, Wu L, Su X, Li Y, Wang K, Li H, Walker D (2019) Rigid aspheric smoothing tool for mid-spatial frequency errors on aspheric or freeform optical surfaces. J Eur Opt Soc Rapid Publ 15:1–9

60. Dong Z, Cheng H, Tam HY (2014) Modified subaperture tool influence functions of a flat-pitch polisher with reverse-calculated material removal rate. Appl Opt 53:2455–2464

61. Walker D, Hsing-Yu W, Yu G, Li H, Zhang W, Lu C (2017) Insight into aspheric misfit with hard tools: mapping the island of low mid-spatial frequencies. Appl Opt 56:9925–9931

62. Chen X, Zhong B, Wang J, Huang H, Deng W, Hou J, Yuan Z, Zhao S (2017) Distortion of removal function based on the local

asphericity of aspheric surface and the viscoelasticity of polishing tool in computer-controlled optical surfacing. Proc Inst Mech Eng C J Mech Eng Sci 232:1135–1145

63. Mehta PK (1990) Pressure distribution under flexible polishing tools: II. Cylindrical (conical) optics. SPIE 1303:189–205

64. Mehta PK, Hufnagel RE (1990) Pressure distribution under flexible polishing tools: I. Conventional aspheric optics. SPIE 1303:178–188

65. Nie X, Li S, Shi F, Hu H (2014) Generalized numerical pressure distribution model for smoothing polishing of irregular midspatial frequency errors. Appl Opt 53:1020–1027

66. Nie X, Li S, Hu H, Li Q (2014) Control of mid-spatial frequency errors considering the pad groove feature in smoothing polishing process. Appl Opt 53:6332–6339

67. Feng Y, Wu H, Cheng H (2016) Tool removal function modeling and processing parameters optimization for bonnet polishing. Int J Optomechatronics 10:141–153

68. Walker DD, Brooks D, King A (2003) The 'Precessions' tooling for polishing and figuring flat, spherical and aspheric surfaces. Opt Express 11:959–964

69. Wang C, Wang Z, Yang X, Sun Z, Peng Y, Guo Y, Xu Q (2014) Modeling of the static tool influence function of bonnet polishing based on FEA. Int J Adv Manuf Technol 74:341–349

70. Li H, Walker D, Yu G, Zhang W (2013) Modeling and validation of polishing tool influence functions for manufacturing segments for an extremely large telescope. Appl Opt 52:5781–5787

71. Li H, Yu G, Walker D, Evans R (2011) Modelling and measurement of polishing tool influence functions for edge control. J Eur Opt Soc Rapid Publ 6:1–6

72. Su X, Ji P, Liu K, Walker D, Yu G, Li H, Li D, Wang B (2019) Combined processing chain for freeform optics based on atmospheric pressure plasma processing and bonnet polishing. Opt Express 27:17979–17992

73. Pan R, Zhang Y, Ding J, Huang C, Wang Z (2016) Optimization strategy on conformal polishing of precision optics using bonnet tool. Int J Precis Eng Manuf 17:271–280

74. Wang C, Yang W, Ye S, Wang Z, Zhong B, Guo Y, Xu Q (2014) Optimization of parameters for bonnet polishing based on the minimum residual error method. Opt Eng 53:075108

75. Shahinian H, Hassan M, Cherukuri H, Mullany BA (2017) Fiber-based tools: material removal and mid-spatial frequency error reduction. Appl Opt 56:8266–8274

76. Shahinian H, Mullany B (2019) Polishing spherical BK7 work-pieces with fiber-based tools. Opt Eng 58:0926101–0926107

77. Shahinian H, Cherukuri H, Mullany B (2016) Evaluation of fiber-based tools for glass polishing using experimental and computational approaches. Appl Opt 55:4307–4316

78. Tuell MT (2002) Aspheric optics: smoothing the ripples with semi-flexible tools. Opt Eng 41:1473–1474

79. Wang C, Yang W, Wang Z, Yang X, Sun Z, Zhong B, Pan R, Yang P, Guo Y, Xu Q (2014) Highly efficient deterministic polishing using a semirigid bonnet. Opt Eng 53:0951021–0951029

80. Wang J, Wan Y, Shi C (2012) Rigidity controllable polishing tool based on magnetorheological effect. SPIE 8416:11–16

81. Li X, Wei C, Zhang S, Xu W, Shao J (2019) Theoretical and experimental comparisons of the smoothing effects for different multi-layer polishing tools during computer-controlled optical surfacing. Appl Opt 58:4406–4413

82. Jessica DN, Alan G, Charles K, Michael M (2011) Incorporating VIBE into the precision optics manufacturing process. SPIE 8126:8126131–81261311

83. Liu SW, Wang HX, Zhang QH, Hou J, Chen XH, Xu Q, Wang C (2021) Smoothing process of conformal vibration polishing for mid-spatial frequency errors: characteristics research and guiding prediction. Appl Opt 60:3925–3935

84. Hou J, Liu S, Wang H, Zhang Q, Chen X, Liao D, Zhong B (2021) Research and application on the key techniques of conformal vibration polishing on optics. Optik 242:1–12

85. Zhang J, Xiang Toh AY, Wang H, Lu WF, Fuh JYH (2018) Vibration-assisted conformal polishing of additively manufactured structured surface. Proc Inst Mech Eng C J Mech Eng Sci 233:4154–4164

86. Dieste JA, Fernández-Cuello A, Javierre C, Santolaria J (2016) Conformal polishing approach: Tool footprint analysis. Adv Mech Eng 8:1–14

87. Song C, Zhang W, Shi F, Lin Z, Nie X (2020) Conformal smoothing of mid-spatial frequency surface error for nano-accuracy Continuous Phase Plates (CPP). Sci Rep 10:2579

88. Jessica DN, Alan G, Nathan S, Kate M, Michael M (2013) Advances in freeform optics fabrication for conformal window and dome applications. SPIE 8708:87081501–87081510

89. Jessica DN, Gould A, Dworzanski D, Klinger C, Wiederhold B, Mandina M (2011) Rapid optical manufacturing of hard ceramic conformal windows and domes. SPIE 8016:8016001–8016009

90. Jessica DN, Gould A, Klinger C, Mandina M (2011) High frequency and random motion rapidly smoothes optical surfaces. Laser Focus World 47:71–74

91. Jessica DN, Kate M, Gregory F (2015) Tolerancing an optical freeform surface: an optical fabricator's perspective. SPIE 9578:9578001–9578008

92. Klinger C (2007) Vibe: a new process for high-speed polishing of optical elements. SPIE 10316:1031611–1031614

93. Kim DW, Burge JH (2010) Rigid conformal polishing tool using non-linear visco-elastic effect. Opt Express 18:2242–2257

94. Shu Y, Kim DW, Martin HM, Burge JH (2013) Correlation-based smoothing model for optical polishing. Opt Express 21:28771–28782

95. Song C, Zhang X, Zhang X, Hu H, Zeng X (2017) Improving smoothing efficiency of rigid conformal polishing tool using time-dependent smoothing evaluation model. Photonic Sens 7:171–181

96. Frost F, Schindler A, Bigl F (1998) Ion beam smoothing of indium-containing III-V compound semiconductors. Appl Phys A 66:663–668

97. Fechner R, Flamm D, Frank W, Schindler A, Frost F, Ziberi B (2004) Ion beam assisted smoothing of optical surfaces. Appl Phys A Mater Sci Process 78:651–654

98. Frost F, Fechner R, Ziberi B, Vollner J, Flamm D, Schindler A (2009) Large area smoothing of surfaces by ion bombardment: fundamentals and applications. J Phys Condens Matter 21:224026

99. Kiyohara S, Iwao M, Masaki T, Honda S (1997) Ion beam smoothing of CVD diamond thin films by etchback method. Nucl Inst Methods Phys Res B 121:191–194

100. Vivensang C, Ferlazzo ML, Ravet M, Turban G, Rousseaux F, Gicquel A (1996) Surface smoothing of diamond membranes by reactive ion etching process. Diam Relat Mater 5:840–844

101. Kanaoka M, Takino H, Nomura K, Mori Y, Mimura H, Yamauchi K (2016) Removal properties of low-thermal-expansion materials with rotating-sphere elastic emission machining. Sci Technol Adv Mater 8:170–172

102. Yamauchi K, Mimura H, Inagaki K, Mori Y (2002) Figuring with subnanometer-level accuracy by numerically controlled elastic emission machining. Rev Sci Instrum 73:4028–4033

103. Zhang F, Song X, Zhang Y, Luan D (2009) Figuring of an ultra-smooth surface in nanoparticle colloid jet machining. J Micromech Microeng 19:1–6

104. Bennett JM, Shaffer JJ, Yukio S, Namba Y (1987) Float polishing of optical materials. Appl Opt 26:696–703

105. Soares SF, Baselt D, Black JP, Jungling KC, Stowell W (1994) Float-polishing process and analysis of float-polished quartz. Appl Opt 33:89–95

106. Wang J (2012) Supersmooth polishing with sub-angstron roughness. SPIE 8416:8416091–8416097

107. Wang J (2012) Ultraprecision optical fabrication on fused silica. SPIE 8416:8416201–8841626

108. Peng W, Guan C, Li S (2013) Ultrasmooth surface polishing based on the hydrodynamic effect. Appl Opt 52:6411–6416